Journal of Hydrology 550 (2017) 726–739

Contents lists available at ScienceDirect

Journal of Hydrology

journal homepage: www.elsevier.com/locate/jhydrol

Research papers

Relationships between sea surface temperature anomalies in the Pacific and Atlantic Oceans and South Texas precipitation and streamflow variability

Dorina Murgulet [a,b,*], Murgulet Valeriu [a,b], Richard R. Hay [b], Philippe Tissot [a,c], Alberto M. Mestas-Nuñez [d]

[a] Department of Physical and Environmental Sciences, Texas A&M University-Corpus Christi, United States
[b] Center for Water Supplies Studies, Texas A&M University-Corpus Christi, United States
[c] Conrad Blucher Institute, Texas A&M University-Corpus Christi, United States
[d] Department of Geological Sciences, University of Texas at San Antonio, United States

ARTICLE INFO

Article history:
Received 11 November 2016
Received in revised form 27 March 2017
Accepted 21 May 2017
Available online 25 May 2017
This manuscript was handled by K. Georgakakos, Editor-in-Chief, with the assistance of Ercan Kahya, Associate Editor

Keywords:
ENSO
PDO
AMO
South Texas
Climate impacts
Precipitation and streamflow variability

ABSTRACT

While many studies have described linkages between large-scale climate phenomena and precipitation and streamflow, fewer studies explicitly address the climatic modulations at sub-regional scales. This study quantifies statistically the temporal variability in precipitation and streamflow at a regional scale in the semi-arid area of South Texas associated with three climate indices: El Niño-Southern Oscillation (ENSO), Pacific Decadal Oscillation (PDO), and Atlantic Multidecadal Oscillation (AMO). Results show that ENSO and PDO strongly modulate rainfall during the cold season and, to various extents, streamflow during the cold and warm seasons. In addition, this study shows that in South Texas streamflow is consistently below normal (i.e. means) while precipitation slightly increases during AMO-warm. To different extents, the Pacific and Atlantic sea surface temperature (SST) anomalies show stronger influences on the climate of South Texas when coupled. Droughts are more correlated with La Niña events but these events play a secondary role during PDO-cold. Although the PDO-cold phase is the dominant driver of droughts in this area, our analyses also show that the coupled effect of the PDO-cold/AMO-warm phases significantly increases the intensity of drought conditions to a degree similar to the PDO-cold/La Niña coupled effect. Given its stronger response to climate anomalies, streamflow offers a more effective tool for predicting climate variability impacts on South Texas water resources when compared to precipitation.

© 2017 Elsevier B.V. All rights reserved.

1. Introduction

While the societal impacts of water resource depletion are well documented (Backlund et al., 2008; Karl, 2009; Pachauri et al., 2014; Taylor et al., 2013), it is not yet clear how the effects of climate change will combine with non-climatic factors such as increased water use, land use/land cover changes, and management practices to impact available freshwater resources. Ecological effects along our ocean coastlines as related to changes in riverine inflows are expected to vary (Dai and Trenberth, 2003). While an increase in discharge from the Mississippi River will intensify the frequency of hypoxia in the Gulf of Mexico, the opposite would happen due to higher discharges in Hudson Bay (Parry, 2007).

An emerging body of research shows that precipitation patterns and streamflow across much of the United States are associated with interannual to multidecadal periods of warming and cooling of the surrounding Pacific and Atlantic surface waters. Clark et al. (2014) and Fu et al. (2010) studied the El Niño Southern Oscillation (ENSO) linkages on precipitation and streamflow in the southeastern U.S. region. Hidalgo and Dracup (2001, 2003) acknowledged a possible ENSO – Pacific Decadal Oscillation (PDO) modulation of spring-summer streamflow and rainfall in the upper Colorado River basin and a strong influence of the Atlantic Multidecadal Oscillation (AMO) on cold season precipitation in the northern Rocky Mountains and the upper Colorado River. Enfield et al. (2001) determined that during the AMO warm phase less than normal rainfall occurs in most of the U.S. territory. Additionally, the streamflow response to the AMO's shift in phase was shown to be significant in the upper Mississippi River basin, the northern Rocky Mountain region, and upper Colorado River basin (Rogers and Coleman, 2003). McCabe et al. (2004) estimated that more

* Corresponding author at: Department of Physical and Environmental Sciences, Texas A&M University-Corpus Christi, 6300 Ocean Drive, Corpus Christi, TX 78412, United States.
E-mail address: dorina.murgulet@tamucc.edu (D. Murgulet).

http://dx.doi.org/10.1016/j.jhydrol.2017.05.041
0022-1694/© 2017 Elsevier B.V. All rights reserved.

than 50% of the spatial and temporal variance in multidecadal drought frequency in the U.S. could be attributed to PDO and AMO effects. Research in the Yellowstone basin based on tree ring reconstructions shows that the major drought in the past 250 years in this basin occurred during a warm AMO-PDO cycle (Hidalgo, 2004). In contrast with streamflow studies based on climate indices, a study conducted by McCabe and Wolock (2014) found that the temporal variability of streamflow in several U.S. regions of coherent spatial variability were only weakly associated with climate indices.

Assessment of water resources at the large-regional scale with applications to small-regional scales can be problematic mainly because water uses and climate gradients can be significant at the sub-regional or local scale and are typically not accurately represented (Faurès, 1997). Predictions derived from general circulation models (GCMs) related to the effects of climate change on two of the most important drivers of freshwater inflow to estuaries, precipitation and temperature, are not consistent. The Canadian CGCM1 and the Hadley HADCM2 models for instance, predict future extreme rainfall and runoff events for the Mississippi River but they disagree on both the magnitude and direction of the change (Day et al., 2005; Wolock and McCabe, 1999). Inaccuracies in these predictions for such large-scale river basins are expected to amplify for sub-regional and small-scale areas.

While these types of analyses provide valuable insight, significant gaps still remain (Kuss and Gurdak, 2014; Meixner et al., 2016). Results derived from regional-scale studies lack the level of detail necessary for informed decision-making (Döll and Fiedler, 2007; Taylor et al., 2013), while those from local scales are almost non-existent. We hypothesize that the comprehensive investigation of sub- or small-scale regions is important and that the large-scale ocean atmosphere phenomena (i.e. ENSO, PDO, and AMO) may be significantly modulated by local forcing, such as topography, surface heterogeneity, and coastal and regional water bodies. Therefore, in order to provide the best tools to assess current water resources and proactively mitigate future supply issues, it is important to quantify the potential relationships between large-scale climate indices and river basins at the sub-regional and/or local scale. These objectives have typically not been addressed in previous studies especially using a long historical record (almost a century) of streamflow or precipitation.

This study investigates the intricate problem of linking the response of rainfall and runoff over semiarid catchments in the South Texas region due to large-scale Atlantic and Pacific ocean-atmosphere phenomena from interannual to multidecadal time scales. The specific objectives are to analyze the statistical relationship of ENSO, PDO, and AMO indices (independently and coupled) with precipitation and streamflow. The derived relations are used to ascertain those climate indicators having the most impact on the water resources to improve predictions as part of an integrated water resources management.

Time-series of climate indices based on monthly sea surface temperature (SST), streamflow (raw monthly mean data for 16 stations from 1922 to 2012), and precipitation (raw daily rainfall amount values for 200 stations over a 110-year period) for extended periods were used to investigate interannual, interdecadal and multidecadal oscillations and the subsequent effects on the hydrology of South Texas. Precipitation and streamflow responses to the individual ENSO, PDO, and AMO and combined PDO-AMO and PDO-ENSO influences were analyzed using non-parametric testing. The correlations are quantified for both (cold and warm) seasons and similar temporal phases of the climate indices in this regional watershed. Through these investigations, the individual and coupled effect of climate phenomena on streamflow and precipitation variability, for almost a century, are identified and analyzed from a water resource perspective.

2. Data and methods

2.1. Study area

The area was selected for its geographic location within North America (i.e. on the semi-arid Gulf Coast) and the interaction with seasonal air masses, which affect its unique climate variability (TWDB, 2012). The study area encompasses approximately 23,500 km^2 in South Texas and is delineated by the Nueces and Guadalupe river sub-basins to the North and South, respectively (Fig. 1).

With a large zonal precipitation gradient (<500 mm to the west to >1000 mm to the east, see Fig. 1), the climate is predominantly subtropical (Kim et al., 2013) humid with a regional climate dominated by hot summers and mild winters with occasional severe freezes (mean annual temperatures 23.5 °C). The prevailing southeasterly trade winds bring large quantities of moisture from the Gulf of Mexico, causing South Texas to experience some of the highest atmospheric moisture contents in the U.S. (Norwine et al., 1995).

Commonly, rainfall and evaporation are the main drivers of the flow of rivers and streams in South Texas. There is very information regarding the groundwater discharge to rivers in this area. For the Gulf Coast aquifer outcrop (which includes the study area), there is a general trend of decreasing baseflow from northeast to southwest. The overall lowest baseflow in the state of Texas are estimated for the study area, except for the upper reaches where some of the largest increasing rends are calculated (BEG, 2005). Compared to eastern Texas where mean annual rainfall is nearly 1500 mm and annual evaporation is less than about 1780 mm, western Texas annual evaporation rates can be as high as 2670 mm; whereas, mean annual rainfall is significantly lower, ranging from 200 to 500 mm. Consequently, streams in eastern Texas flow year round while most western Texas streams flow intermittently (TWDB, 1996). For instance, the springs that feed the Comal and San Marcos Rivers, in the north side of the San Antonio river basin, have an average monthly discharge of 8.7 and 4.6 cubic meter per second ($m^3 \cdot s^{-1}$), respectively. During the severe drought of the 1950s the Comal Springs, which are more prone to drought conditions, ceased to flow, while San Marcos River continued to flow, but dropped to 1.3 $m^3 \cdot s^{-1}$ (SAR BBEST et al., 2011). While mostly driven by precipitation patterns that influence the spring flow supporting the river, stream flow can be amplified by treated municipal effluent that originates primarily as groundwater from the Edwards Aquifer (SAR BBEST et al., 2011). Furthermore, the hydrology in the lower part of San Antonio River varies seasonally. In the investigated area, the rainy season is often defined as the months of April-June and September-October with summer/warm (April to September) and winter/cold (October to March) mean monthly rainfall of 72.7 (number of records in months (n) = 620) and 44.9 mm (n = 492), respectively. The highest streamflow months typically extend from July through October. The mean monthly basin-normalized streamflow for the warm and cold months are $1.13 \cdot 10^{-3}$ (n = 444) and $1.12 \cdot 10^{-3}$ $m^3 \cdot s^{-1} \cdot km^{-2}$ (n = 356), respectively.

2.2. Data

The major data sets used to develop the relationships between South Texas streamflow, precipitation, and SST variability were surface flow discharge from streams unimpaired by dams and barriers, daily precipitation data in the study area, and SST data for the Pacific (ENSO 3.4 and PDO) and Atlantic Oceans (AMO).

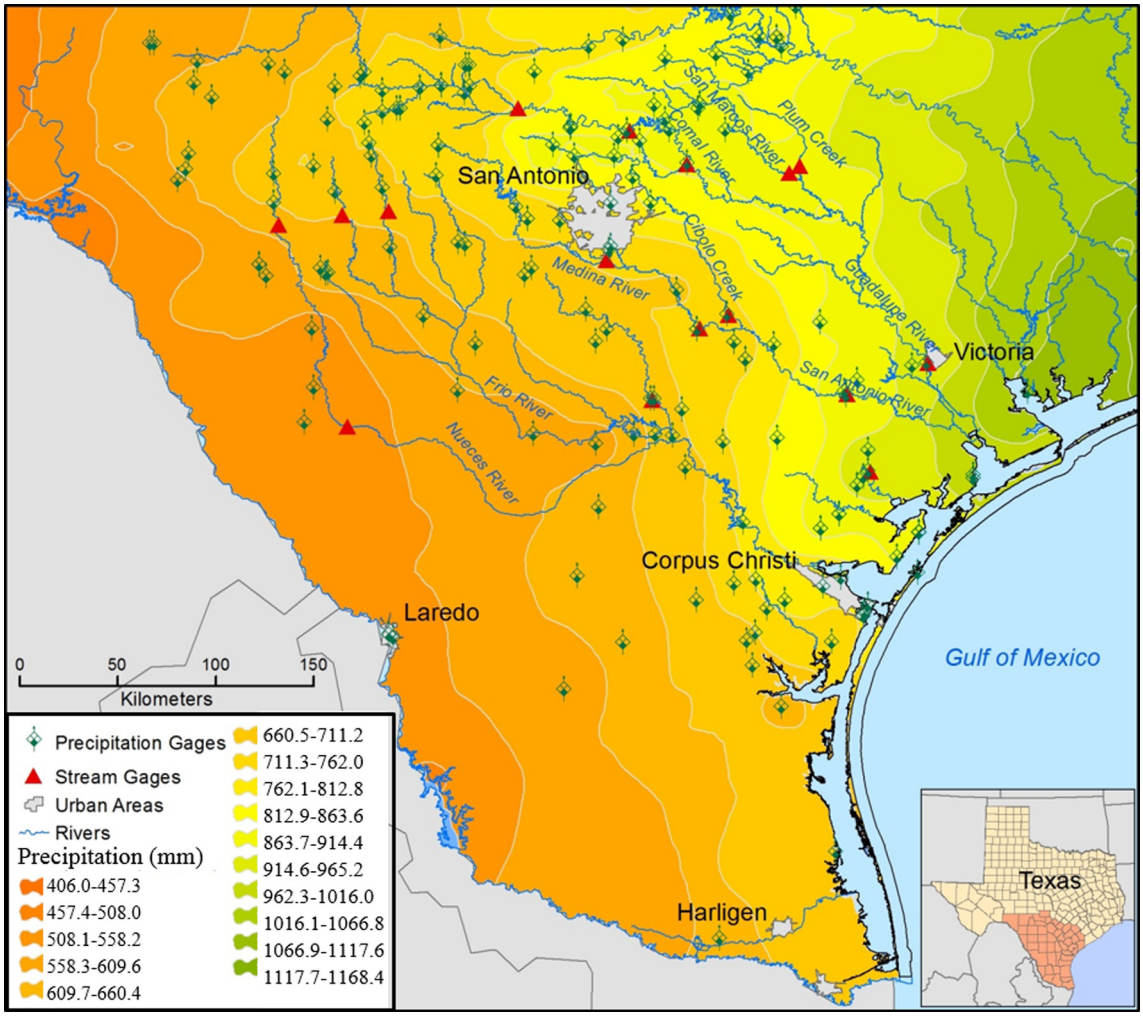

Fig. 1. Change in total annual precipitation rates (in millimeters (mm)) from east to west are derived from the annual average rainfall for the period of record. The location of the study area is depicted by the highlighted area in the lower-right inset Texas map. The locations of stream and precipitation gauges as well as the stream system analyzed in this study are also represented.

2.2.1. Streamflow and precipitation data

Daily streamflow data from 16 unimpaired gage stations were identified in the Guadalupe, San Antonio and Nueces River basins utilizing the U.S. Geological Survey (USGS) NWIS web data retrieval [http://waterdata.usgs.gov/nwis/]. For several streams, stations upstream from dams and barriers were included while stations downstream from the impairment were not. While water withdrawals likely affect all streams they were not considered impairments in this study, their impact is addressed as part of the results and discussion sections. The period of record for all stations extended from 1922 to 2012 (90 years). Daily atmospheric precipitation data from approximately 200 meteorological stations in the South Texas area were collected from the National Oceanic and Atmospheric Administration (NOAA), National Climatic Data Center (NCDC) web site: http://www.ncdc.noaa.gov/. The data were imported to ArcGIS and spatially interpolated (in average 60%) using the ordinary kriging method on daily data. The same method was utilized to interpolate the missing data in the precipitation time-series of each station. Remaining data gaps were filled in assuming that precipitation rates change linearly in space and time. However, although the number of active precipitation stations were less at the beginning of the record when compared to mid-record, most of the interpolated data is derived from station discontinuation and replacement with others located within a few hundred of meters from the original location in order to maintain a continuous record.

2.2.2. Pacific and Atlantic sea surface temperature data

2.2.2.1. Pacific Decadal Oscillation. The PDO index is defined as the leading principal component of monthly SST anomaly variability in the North Pacific Ocean, poleward of 20°N (Mantua et al., 1997). Updated, standardized values for the PDO index data were retrieved from Nate Mantua's anonymous ftp site [http://research.jisao.washington.edu/pdo/PDO.latest]. This index is derived from two data sources: UKMO Historical SST data set for 1900-81 including Reynold's Optimally Interpolated SST (V1) values for January 1982 – December 2001, and the OI SST Version 2 (V2) beginning January 2002 – present.

2.2.2.2. Atlantic Multidecadal Oscillation. The AMO index, an index of the North Atlantic SST as defined by Enfield et al. (2001), was acquired from NOAA's Earth System Research Laboratory (ESRL) web page available at http://www.esrl.noaa.gov/psd/data/timeseries/AMO/. The AMO index time-series (both smoothed and unsmoothed versions) are based on the monthly updated Kaplan SST dataset (Kaplan et al., 1998; Reynolds and Smith, 1994). Kaplan SST V2 data comes from the NOAA/OAR/ESRL PSD, Boulder, Colorado, USA, from their web site at http://www.esrl.noaa.gov/psd/.

The spatial coverage is 5.0-degree latitude by 5.0-degree longitude (5° × 5°) and the temporal coverage consists of monthly anomalies relative to the 1951–1980 climatological base period. A complete description of the originator's data set is available at http://ingrid.ldeo.columbia.edu/SOURCES/. KAPLAN/.EXTENDED/.v2/.ssta/.

2.2.2.3. El Niño-Southern Oscillation. The ENSO monthly index used in this study is based on area-averaged SST anomalies in the Niño 3.4 region (120°W–170°W and 5°S–5°N) of the tropical Pacific Ocean and was retrieved from the National Center for Atmospheric Research Climate Analysis as five month running means relative to a base period climatology from 1950–1979 (Trenberth, 1997).

2.3. Methods

2.3.1. Streamflow and rainfall data preprocessing

The monthly arithmetic mean of the regional precipitation was used to generate the cold and warm season precipitation indices (Fig. 2a) which are November to February and May to September, respectively. The monthly streamflow rates ($m^3 \cdot s^{-1}$) were normalized to the respective basin area and the calculated geometric mean values (in $m^3 \cdot s^{-1} \cdot km^{-2}$) were used in the following analysis.

The monthly flow records were used to generate annual cold and warm season indices for each stream (Fig. 2b) that correspond to the streamflow total for each season. Annual data are used to avoid any interpretative bias due to autocorrelations caused by seasonal changes. For both precipitation and streamflow, the months of March, April, and October are considered transitional months and their records are shown in Fig. 2, but are not included in the statistical analyses presented here.

2.3.2. SST data preprocessing and phase definition

To define the phases of the SST indices low-pass filtering of the raw monthly ENSO, PDO and AMO SST indices were performed using 12, 60, and 120 month sliding windows, respectively. These smoothing operations respectively reduce intraseasonal, interannual, and interdecadal effects ("noise") in these time series. Overall, the SST phases (warm/positive and cold/negative) were defined according to the sign of these smoothed ENSO, PDO, and AMO indices, which are shown in Fig. 3.

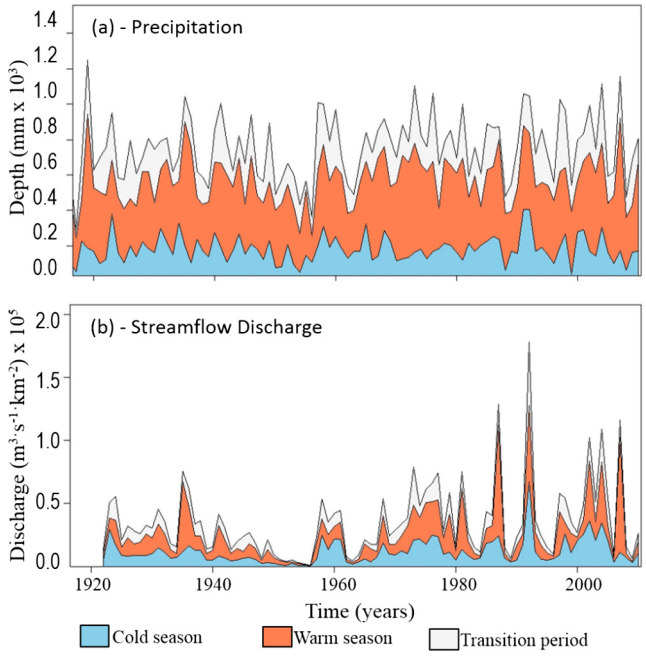

Fig. 2. Stacked area chart showing how each category (i.e. cold, warm, and transition months) contribute to the cumulative total of annual: (a) precipitation depths and (b) streamflow discharge volumes. The variables are temporally sectioned in cold (November-February) and warm (May-September) seasons as well as a transition period (March, April, October) not used in the statistical analyses.

The positive/negative phases of the ENSO index to respective El Niño (ENSO warm)/La Niña (ENSO cold) events is simple but does not separate the intermediate (ENSO neutral) transition stages. Thus, a more restrictive definition of El Niño/La Niña that takes into account persistence was also used following the recommendation of Trenberth (1997). Briefly, ENSO index was smoothed using a 5-month running mean (from the original source) and a 6-month persistence warm/cold phase was required (i.e. to be above/below +/- 0.4 °C for 6 months or more) to qualify as an El Niño/La Niña event. With this definition, El Niño/La Niña events occur roughly about 50% of the time (Trenberth, 1997).

The PDO and AMO periods between 1926 and 1994 are adopted from McCabe et al. (2004) which evaluated coupled effects of PDO and AMO for four periods: 1- PDO warm/AMO warm (1926–1943); 2 - PDO cold and AMO warm (1944–1963); 3 - PDO cold and AMO cold (1964–1976), and 4 - PDO warm and AMO cold (1977–1994). Our evaluation of records and recent studies (Gray et al., 2004; Maurer et al., 2004; McCabe et al., 2004) indicate that PDO returned to a warm phase in 1995 before shifting back from the warm phase to the cold phase around 2000. After 2000 PDO shifted quickly back to a warm phase for a few years, and, starting with 2005, then returned to a cold phase that is apparent at least until 2012. AMO shifted to the warm phase in the mid-nineties and stayed in that phase for the rest of the study period. Therefore, we categorize PDO/AMO warm and cold years, for the remaining record (1996–2012) of oceanic SSTs as: 1 – PDO warm/AMO warm (1996–1998 and 2002–2005); and 2 – PDO cold and AMO warm (1998–2002 and 2006–2012).

2.3.3. Statistical analysis

To investigate statistical relations a cross-correlation function (ccf) analysis was performed. Cross (lagged) correlation provides an effective measure to establish the similarity of two variables as a function of the time-lag of one relative to the other. We only discuss correlation coefficients ("r" not "R^2") that are significant at the 95% confidence level. The ccf were constructed using the climate indicator as the preceding/input "x" time-series and precipitation (or streamflow) as the trailing/response "y" time-series. For the precipitation and streamflow cross-correlation, precipitation was used as the preceding time-series. The purpose of doing lagged correlations between rainfall and streamflow is to investigate the response time of river runoff to precipitation events. Since we are working with monthly data and surface runoff generally responds to rainfall rapidly (hours to days) a maximum of the lagged correlation function is expected at zero lag. Slower response times of streamflow to rainfall are expected under dry soil conditions (days to months) when rainfall leads streamflow. In this study, lagged correlations between rainfall/streamflow and the climatic indices are explored only for small lags (∼months for ENSO and ∼years for decadal and multidecadal). Because the climatic indices used are low-passed (smoothed) in time to remove variabilities at intraseasonal (12 month filter), internanual (60 month filter), and interdecadal (120 month filter) time scales for ENSO, PDO, and AMO, respectively, we are cautious to interpret these lagged correlations as more than a rapid response.

To minimize the effect of autocorrelation in the "x" time-series, the well-established prewhitening method was applied to both time-series (Chatfield, 2016; Jensen, 1996). Prewhitening was achieved by finding an autoregressive integrated moving average (ARIMA) model that best fit the "x" time-series and replacing the

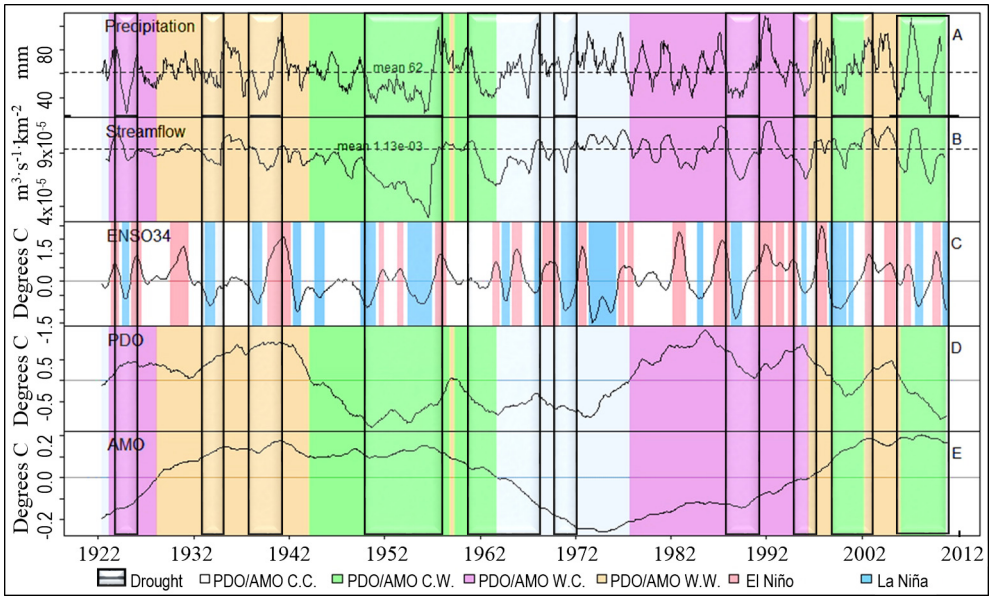

Fig. 3. Graph showing the: (A) precipitation (12 month filter), (B) streamflow (12 month filter), (C) ENSO 3.4 (12 month filter), (D) PDO (60 month filter), and (E) AMO (120 month filter) over the entire period of study. PDO and AMO coupled cycles of the warm and cold phases are depicted by different shaded zones. Recorded Texas droughts (TWRI, 2011) are represented by vertical transparent boxes.

"x" time-series with the residuals from the ARIMA model. To determine which ARIMA model was the best fit, all combinations (from zero to four) of the three order components (autoregressive order, degree of differencing, and moving average order) were tested. The model with the lowest Akaiki information criteria (AIC) value was selected as the best fit. The "y" time-series was then replaced with the residuals produced by applying the best fit "x" time-series ARIMA model to the "y" time-series. ARIMA modeling was performed with the R Project for Statistical Computing software using the Hyndman "forecast" library (Hyndman, 2008). Further discussion of ARIMA modeling can be found elsewhere (Anderson, 1977; Box et al., 2015; Salas et al., 1980).

An independent evaluation of the Pacific (Atlantic) Ocean SSTs impacts on South Texas precipitation and streamflow variability was performed using the cold or warm phases of the ENSO (i.e. ENSO cold and warm years as well as the more restrictive El Niño and La Niña years), PDO cold years (AMO cold years), and the PDO warm years (AMO warm years). The respective cross-correlations between two series (i.e. annual means) were examined in order to identify the statistical significance (Mann-Whitney-Wilcoxon test) of the relationships between precipitation and streamflow and the climate variability indexes.

The Mann-Whitney-Wilcoxon test (Fisher, 1958, 1973), a rank--sum test rather than a test of the mean applied to check for identical populations (does not require normal distribution), was utilized to evaluate and quantify the impacts of SSTs on streamflow and precipitation variability during cold and warm season. The use of this test was necessary as a Shapiro-Wilk test for normality (null hypothesis is normal distribution) showed that data are not normally distributed. The Mann-Whitney-Wilcoxon test was applied to cold and warm phases of each of the interdecadal (AMO and PDO cold and warm) and interannual (ENSO cold and warm phases) STTs in relation to the precipitation and streamflow cold and warm water years. The ENSO variability was also analyzed using the more restrictive El Niño and La Niña phases, which span over shorter periods compared to the cold and warm ENSO phases.

Using this method, we tested different hypothesis with the significance of the results quantified using the p-value. Following the common convention, if the p-value is less than (or equal to) α, then the null hypothesis is rejected in favor of the alternative hypothesis. If the p-value is greater than α, which at 95% is commonly 0.05, then the null hypothesis is not rejected. Although we use a 95% significance level, most p-values used in selecting different populations to quantify climate variability are well below 0.05, thus ensuring a much greater level of statistical significance.

The coupled effects of PDO and AMO and PDO and ENSO on precipitation and streamflow have been analyzed using the same above-mentioned techniques. To measure the variability of precipitation and streamflow in response to individual and coupled SSTs anomalies, we have computed the percent (%) yearly and seasonal (i.e. cold and warm water years) difference in precipitation depths and streamflow discharge volumes with respect to all temporal interdecadal and interannual phases. For these calculations, we used mean values (Giorgi et al., 2001) which does not exclude the influence of extreme events such as drought or wet periods, and calculated percent decrease or increase in precipitation and streamflow for the respective coupled phases of the climate indicators. .

The relationship between the SST anomalies and drought occurrence also was analyzed using non-parametric testing such as the chi-squared (Cohen, 1988; Cramér, 1946; Nist/Sematech, 2012; Snedecor and Cochran, 1989) and Cramer's "V" methods (Cramér, 1946). These techniques are a measure of both the statistical significance and strength of association between variables. The significance of correlation is based on p-values as mentioned above while the strength of correlation is measured using "V" values or levels of association. For instance, "V" values between 0.15 and 0.20 indicate that variables are only weakly correlated and minimally acceptable, while values between 0.35 to 0.40 show very strongly/desirable correlated variables (Cohen, 1988). We have calculated drought scores (DS) using the ratio of reported non-droughts to droughts months (TWRI, 2011) that were statistically associated with each temporal phase of the climate indicators. We consider that any score value lower than one is associated with a potential occurrence of drought and the probability becomes stronger as the score approaches 0.1. This is based on the assumption that, in any given year or SST phase, drought occurrence is likely when the number of dry months exceeds that of wet months.

3. Results

3.1. South Texas precipitation and streamflow variability

A cross-correlation comparison between the monthly time-series of precipitation and stream flow is presented in Fig. 4 (precipitation leads for negative lags). The horizontal dashed lines show the critical correlation value (0.06) at the 95% significance level. A significant maximum positive correlation (0.41) exists at zero lag, which is consistent with a transfer of rainfall and surface runoff to the rivers following significant precipitation events. Other smaller but significant positive correlations occur for lags between −1 and −8 months, likely the delayed response of streamflow to that portion of precipitation that becomes part of aquifer storage and discharges as baseflow (subsurface) to rivers and streams. In addition to the processes introduced here to describe the relation between precipitation and streamflow discharge, there are likely other factors within a basin that can influence this relationship (Prathumratana et al., 2008), and those will be addressed in the discussion section.

The rank- sum test shows that precipitation during the warm-water years is almost twofold higher when compared to the cold years, while streamflow discharge is only slightly higher during the cold years (Fig. 5; Tables 1, 2). This could be explained by losses to evaporation which in semi-arid and arid regions could exceed precipitation rates during the warm months (IPCC, 2007). In addition, increased water uses, from both riverine and groundwater sources, during the warm months may significantly decrease discharge to streams/rivers. Differences in medians reveal statistically significant variabilities in precipitation between the cold and warm season precipitation (p-value $1.4 \cdot 10^{-21}$). On the other hand, seasonal streamflow variability is only marginally significant (p-value $9.0 \cdot 10^{-3}$) (Table 1).

3.2. ENSO and South Texas precipitation and streamflow

Cross-correlation analysis indicates significant positive correlations between ENSO and precipitation at lag zero months (r = 0.4; c.i. of 0.19), likely due to a strong positive correlation that occurs during the cold season (r = 0.35). Rank-sum test analyses of the El Niño and La Niña phases of ENSO indicate a slightly higher influence on the annual precipitation (p-value: $7.9 \cdot 10^{-10}$; variability: 29.0%) when compared to the cold and warm ENSO phases (p-value: $2.05 \cdot 10^{-8}$; variability: 18.8%). This may be explained by the neutral interval of ENSO included in the ENSO cold and warm analyses. El Niño causes an increase above the overall/seasonal mean and La Niña a decrease. Both ENSO cold and warm and El Niño and La Niña phases have a significant influence on the cold season precipitation (p-values: $1.6 \cdot 10^{-8}$ and $7.1 \cdot 10^{-11}$, variability: 53.7% and 34.4%, respectively), while no effects on the warm season precipitation (p-value: 0.94 and 0.7 respectively) (Fig. 6a, b; Table 1). This is also confirmed by the insignificant cross-correlations.

The rank-sum test results also show that ENSO cold/warm and El Niño/La Niña phases significantly modulate yearly streamflow discharge (p-value: $1.7 \cdot 10^{-8}$ and $6.7 \cdot 10^{-6}$, variability: 34.7% and 49.9%, respectively) (Fig. 6a, b). Furthermore, El Niño and La Niña cause 57.2% of seasonal discharge variability during the cold season and 48.1% during the warm season. A high impact is also computed for the cold season streamflow (47.7%) during the ENSO cold/warm phases, although there are no significant correlations. A much lower variability (20.5%) was estimated during the warm season when compared to the El Niño/La Niña (Table 1; Fig. 6a, b).

3.3. PDO and South Texas precipitation and streamflow

PDO positively correlates with yearly precipitation at zero lag years (r = 0.34; c.i. = 0.19). A relatively weak negative lag correlation at −3 years (r = −0.21) that can be associated with PDO cold when less precipitation is expected to occur. These lagged effects are evident during the warm season as indicated by the strong negative correlation (r) of −0.25 at lag −3 years. Statistical evaluation of precipitation variability shows that the cold and warm phases of PDO have no significant impact on the yearly precipitation depths (p-value = 0.14; medians: 49.4 and 53.0 mm, respectively). On the other hand, the cold season precipitation is slightly higher during

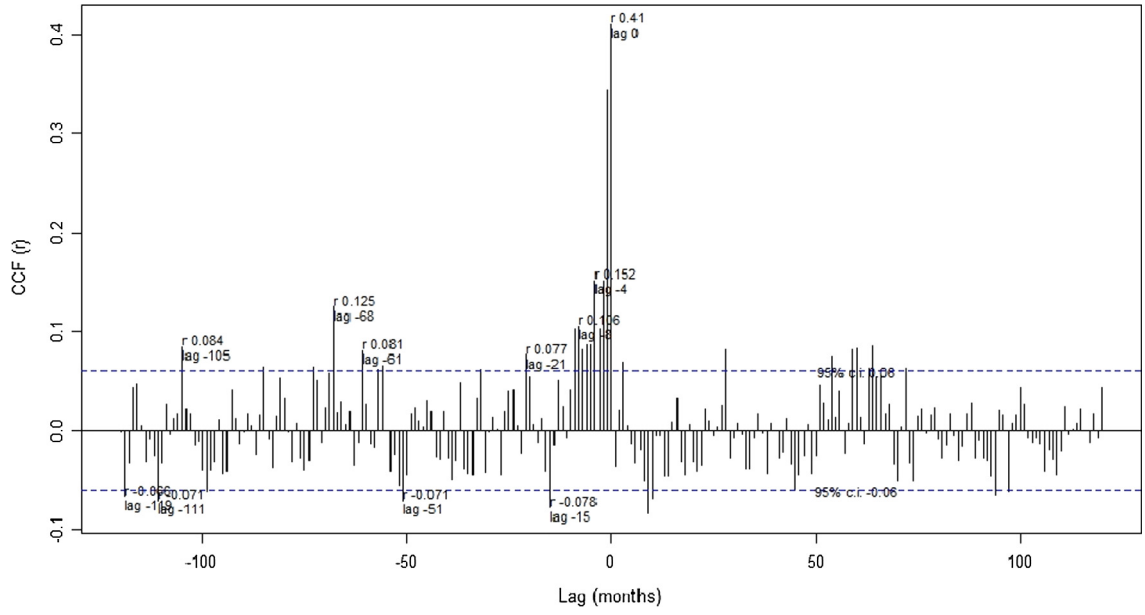

Fig. 4. Cross correlation function between precipitation and streamflow (precipitation leads for negative lags). A strong autocorrelation is noted showing the positive response of streamflow to precipitation events. Critical correlation values (c.i.) are represented by horizontal dashed lines and are a function of the number of records/data points. As the lag is increased to compute lagged correlations, the number of data points is reduced, thus the uncertainty in the sample autocorrelation increases. As a result, correlations at larger lags are not considered in this paper.

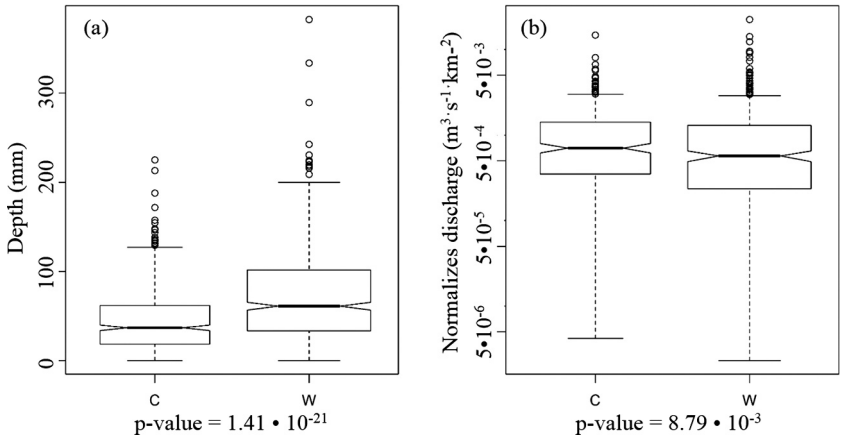

Fig. 5. Boxplot analyses of monthly (a) precipitation and (b) streamflow showing the statistically significant differences between precipitation and streamflow discharge during the cold (C) and warm (W) seasons (p-value from Mann-Whitney-Wilcoxon test).

Table 1
Summary of precipitation and streamflow changes. Values are reported as% above (+) or below (−): the overall mean for annual data, the cold season mean, and warm season mean for different periods composited according to the phases of the climatic indices. The number of records/months (months) included in the variability estimates for each climate anomaly and precipitation and streamflow are included in parenthesis next to the percent value.

Climate indices	Precipitation (%); number of data points "n" (months)			Streamflow (%); number of data points "n" (months)		
	Annual	Cold season	Warm season	Annual	Cold season	Warm season
ENSO						
Cold	−9.2 (758)	−15.6 (240)	−0.5 (250)	−16.9 (551)	−20.9 (200)	−10.9 (209)
Warm	+9.6 (725)	+18.8 (202)	+0.5 (305)	+17.8 (514)	+26.8 (156)	+9.6 (235)
ENSO						
La Niña	−13.6 (359)	−22.9 (113)	−3.2 (105)	−15.4 (250)	−14.5 (97)	−21.0 (90)
El Niño	+15.4 (453)	+30.8 (147)	+3.0 (172)	+34.5 (308)	+42.7 (110)	+27.1 (128)
PDO						
Cold	+1.5 (613)	−8.7 (201)	+5.6 (258)	−19.5 (509)	−16.9 (168)	−21.4 (213)
Warm	+5.4 (688)	+9.7 (231)	+2.9 (286)	+17.6 (556)	+15.1 (188)	+19.7 (231)
AMO						
Cold	−2.2 (772)	−4.7 (246)	−2.0 (305)	+13.3 (466)	+13.4 (156)	+12.3 (194)
Warm	+2.4 (711)	+5.2 (196)	+2.1 (205)	−10.1 (599)	−9.9 (200)	−9.4 (250)
PDO/ENSO						
Cold/Cold	−5.5 (374)	−21.0 (140)	+8.6 (135)	−17.2 (314)	−19.4 (117)	−14.2 (115)
Warm/Cold	−3.6 (281)	−4.4 (97)	+3.2 (110)	−16.4 (237)	−23.1 (83)	−6.9 (94)
Cold/Warm	+12.2 (239)	+19.2 (61)	+2.3 (123)	−23.1 (195)	−11.1 (51)	−29.7 (98)
Warm/Warm	+11.6 (407)	+20.0 (134)	+2.7 (176)	+42.5 (319)	+45.3 (105)	+37.7 (137)
PDO/AMO						
Cold/Cold	+5.8 (286)	−9.5 (97)	+13.9 (120)	+10 (178)	+8.6 (60)	+7.9 (75)
Warm/Cold	+1.2 (420)	+7.3 (139)	−3.9 (174)	+15.4 (288)	+16.4 (90)	+15.1 (119)
Cold/Warm	−2.2 (327)	−7.9 (104)	−1.4 (138)	−35.3 (331)	−30.6 (108)	−37.0 (138)
Warm/Warm	+11.8 (268)	+13.3 (92)	+13.5 (112)	+20 (268)	+13.8 (92)	+24.6 (112)
Precipitation/Streamflow	N/A (1483)	−24.9 (492)	+21.5 (620)	N/A (1065)	−0.3 (356)	+0.6 (444)
p-value		$1.4 \cdot 10^{-21}$			$9.0 \cdot 10^{-3}$	

PDO-warm (median: 49.2 mm versus 41.0 mm) (p-value = 0.005). An approximately 18.4% change in precipitation between the cold and warm phases of PDO is likely for South Texas during the defined cold season years, while no significant influence of PDO is observed on the warm season precipitation (p-value = 0.67) (Fig. 6c). This is consistent with the cross-correlation evaluation which shows no significant teleconnections for the warm season but a significant positive link for the cold season (lag zero; r = 0.27).

Significant positive correlations between PDO and annual streamflow (r = 0.24; c.i. = 0.21) occur at lag zero showing a rapid streamflow response especially during the warm season (r = 0.22). Contrary to precipitation, yearly streamflow seems to vary significantly with the cold and warm phases of PDO (p-value of $3.4 \cdot 10^{-14}$) (Table 1) causing a 37.1% total change. Furthermore, the cold and warm season streamflow also shows significant changes between the cold and warm phases of PDO as indicated by the differences in means and medians (Table 2) and sufficiently low p-values (i.e. $3.2 \cdot 10^{-6}$ for cold season and $6.6 \cdot 10^{-6}$ for warm season). For the period of record, PDO caused a total change of 32.0% in cold season streamflow and 41.2% in the warm season (Fig. 6c).

3.4. AMO and South Texas precipitation and streamflow

The AMO cold and warm phases do not modulate yearly and seasonal precipitation (p-value: 0.26). Based on the slight differences of the means, percentage changes in year-to-year and seasonal precipitation are extremely low (Tables 1, 2; Fig. 6d) and are not statistically significant. Cross-correlations show that precipitation leads AMO (i.e. significant positive correlation at lag −4 years (r = 0.22; c.i. 0.19 and decreasing with time)) for the warm season in contrast with the North Pacific climate anomalies influencing South Texas precipitation mainly during the cold season. However, PDO and ENSO correlations are at the zero lag and are stronger, showing a significant immediate impact of these

Table 2
Summary table of mean and median values for each temporal phase of individual and coupled climate indicators and defined water years/seasons used in the statistical analyses. Mean monthly rainfall and normalized streamflow are reported in *mm* and $10^{-4} \cdot m^3 \cdot s^{-1} \cdot km^{-2}$, respectively.

SST anomaly	Monthly precipitation		Cold season precipitation		Warm season precipitation		Monthly streamflow		Cold season streamflow		Warm season streamflow	
	mean	median	mean	median	mean	median	Mean	median	mean	median	mean	median
PDO/ENSO												
Cold/Cold	56.5	45.1	35.4	30.5	78.9	66.8	9.3	4.3	9.0	4.3	9.7	4.0
Warm/Cold	57.6	46.9	42.9	36.5	75.0	63.8	9.4	6.6	8.6	7.0	11.0	5.8
Cold/Warm	67.1	59.4	53.5	55.5	74.3	65.4	8.7	5.4	10.0	5.9	8.0	4.6
Warm/Warm	66.8	55.5	53.9	47.4	74.6	59.3	16.0	10.0	16.0	10.0	16.0	8.5
PDO/AMO												
Cold/Cold	63.3	50.1	40.6	35.4	82.7	69.4	12.0	7.3	12.0	6.8	12.0	7.0
Warm/Cold	60.5	50.9	48.2	41.4	69.8	57.2	13.0	7.1	13.0	8.0	13.0	5.6
Cold/Warm	58.5	48.1	41.3	35.2	71.6	65.0	7.3	3.3	7.8	3.6	7.1	2.9
Warm/Warm	66.9	55.5	50.9	43.7	82.5	71.7	14.0	8.7	13.0	9.2	14.0	7.9
PDO												
Cold	60.7	49.4	41.0	35.4	76.7	65.9	9.1	4.8	9.3	4.7	8.9	4.3
Warm	63.0	53.0	49.2	41.6	74.8	61.5	13.0	8.1	13.0	8.4	14.0	6.8
AMO												
Cold	58.5	48.2	42.8	36.4	71.2	58.4	13.0	7.2	13.0	7.5	13.0	6.3
Warm	61.2	49.7	47.2	39.2	74.2	64.7	10.0	6.0	10.0	6.7	10.0	5.0
ENSO												
Cold	54.3	42.9	37.9	30.7	72.3	61.5	9.4	5.5	8.9	6.3	10.0	4.7
Warm	65.5	55.4	53.3	45.8	73.0	60.8	13.0	8.3	14.0	9.4	12.0	6.6
ENSO												
La Niña	51.7	40.6	34.6	27.9	70.4	61.8	9.5	5.2	9.6	5.9	9.0	4.1
El Niño	69.0	59.4	58.7	54.0	74.8	62.5	15.0	8.5	16.0	9.4	14.0	6.3
All years	59.8	48.8	44.9	36.8	72.7	61.2	11.0	6.7	11.0	7.1	11.0	5.7

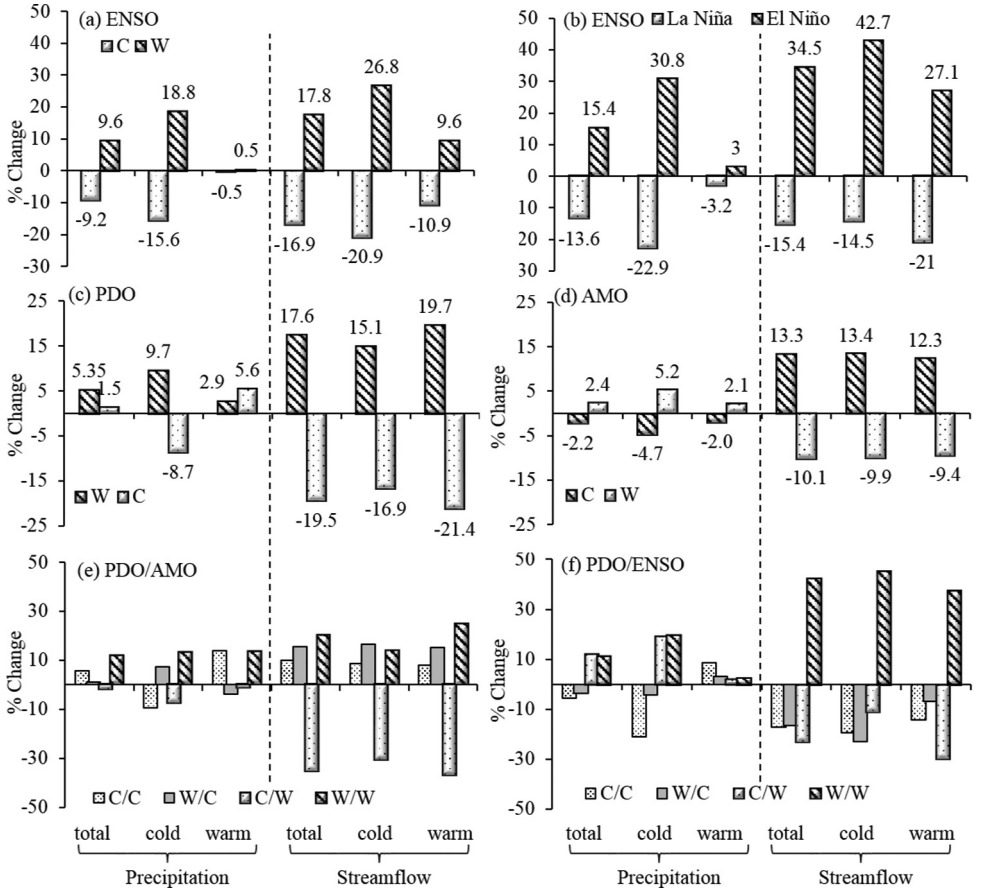

Fig. 6. Graphs showing the computed% changes in precipitation and streamflow during ENSO warm and cold phases (a), La Niña and El Niño (b), PDO (c), AMO (d), coupled PDO/AMO (e), and coupled PSO/ENSO (f).

anomalies that may explain the large observed precipitation variabilities when compared to AMO.

The overall streamflow response to the AMO is significant (p-value of $8.6 \cdot 10^{-5}$) with a total variability of 23.6% between the two AMO phases (Fig. 6d). Seasonally, streamflow is slightly higher during the AMO-cold compared to AMO-warm (p-value: 0.02; Table 1), despite the lack of influence of the climate indices (AMO -cold and -warm) on precipitation. Cold and warm season streamflow discharge could vary by about 23.2% and 22.6%, respectively, between the two AMO phases (Fig. 6d). A weak, but statistically significant positive correlation at lag −4 years (r = 0.22; c.i. 0.21) is also noted for the warm season which likely reflects the offset effects of AMO on precipitation and, thus, streamflow response.

3.4.1. PDO-AMO coupled influences

3.4.1.1. Precipitation variability. Coupled PDO cold/AMO cold (PDO/AMO C/C), PDO warm/AMO cold (PDO/AMO W/C), and PDO cold/AMO warm (PDO/AMO C/W) phases show little difference in median values. The overlapping confidence intervals (95%), which are insensitive to distribution, provide strong evidence that they are not independent populations. A slight difference is noted for the PDO warm/AMO warm (PDO/AMO W/W) when compared to the other conditions, with a lower degree of overlapping of the 95% c.i. (Fig. 7a).

A Mann-Whitney-Wilcoxon test performed between the W/W and the other phases shows no significant statistical differences between the W/W and the C/C and W/C cycles (p-value range between 0.1 and 0.9). On the other hand, slightly significant differences at the 95% c.i. are found between the W/W and C/W cycles (p-value: 0.02) indicating that these could be independent populations when compared to the other two coupled PDO/AMO cycles. The computed annual precipitation variability (expressed as% below or above the overall precipitation mean presented in Table 1) indicate that the combination of same sign PDO and AMO have the largest effect on South Texas precipitation, with the largest influence during the PDO/AMO W/W (11.8% above mean), followed by the PDO/AMO C/C (5.8% above the mean).

Although following the same pattern as the yearly trend, slightly higher climatic seasonal variability is noted for precipitation among the different PDO/AMO phases (Fig. 7c, Table 2). Significant differences at the 95% c.i. are observed for the cold season precipitation during the following coupled phases: C/C and W/W (p-value: 0.02) and the C/W and W/W (p-value: 0.01). An increase above the cold season mean precipitation is estimated to occur during the PDO/AMO W/W (13.3%) and W/C (7.3%) cycles and a decrease below the mean during the coupled PDO/AMO C/C (9.6%) and C/W (7.9%) (Table 1). Significant differences in warm season precipitation medians at the 95% c.i. are noted for the PDO/AMO W/C and W/W (p-value: 0.04) and for the C/C and C/W (p-value: 0.01; Fig. 7d). Similar to the yearly effects, the most significant variabilities in the warm season precipitation are estimated for the C/C and W/W coupled phases when precipitation is expected to be above the warm season mean (13.9% and 13.5%, respectively). Only weak influences (i.e. decrease) on precipitation are expected during the warm season when PDO and AMO are of opposite signs (i.e. 3.9% and 1.4% below the mean (Table 1)).

3.4.1.2. Streamflow variability. There is almost no difference in streamflow medians, both annual and seasonal, among the coupled AMO/PDO C/C, W/C, and W/W phases (Table 2) and the overlapping confidence intervals indicate that they are not independent populations (Fig. 7b). On the other hand, the C/W condition shows a markedly different median and no overlapping confidence intervals (likely independent datasets), with significant statistical differences, compared to the other coupled PDO/AMO phases (p-values: annual = $2.2 \cdot 10^{-21}$ to $1.0 \cdot 10^{-2}$; cold season = $2.4 \cdot 10^{-7}$ to $3.1 \cdot 10^{-4}$; warm season: $2.1 \cdot 10^{-10}$ to $2.9 \cdot 10^{-2}$). As a result, annual streamflow discharge rates are likely to exceed the overall mean during the C/C (10.0%), W/C (15.4%), and W/W (20.0%), while dramatically decreasing below the mean during the C/W coupled phase (35.3%) (Table 1; Fig. 7e). Only slightly lower variability is estimated to occur for the cold season streamflow when compared to the respective mean. The highest variability is estimated to occur during the warm season, especially during the C/W (37.0% lower than the respective mean) and the W/W (24.6% above the mean) phases (Fig. 7e, Table 2).

3.4.2. PDO-ENSO coupled influences

3.4.2.1. Precipitation variability. Precipitation medians show no variability during the PDO/ENSO combined phases with the same sign of ENSO (Table 1, Fig. 8a). Although the overlapping confidence intervals are evidence that all four-phase combinations are dependent populations, the two groups, classified based on the ENSO sign (i.e. ENSO cold/negative and warm/positive), are statistically different. The Mann-Whitney-Wilcoxon test was applied to check the statistical difference between the respectively coupled conditions. The combination of conditions C/C-W/W, W/C-W/W, W/C-C/W, and C/C-C/W, are statistically different with sufficiently low p-values ($5.2 \cdot 10^{-5}$, $3.2 \cdot 10^{-3}$, $1.0 \cdot 10^{-2}$, and $5.7 \cdot 10^{-4}$, respectively). These statistically relevant combinations are included in the estimation of yearly precipitation changes (expressed as% below or above the overall precipitation mean presented in Table 2) indicating that the largest variabilities occur when ENSO is warm (C/W and W/W: 12.2% and 11.6% above the mean, respectively) (Fig. 8a).

Similar to the annual results, cold season precipitation shows significant differences among the combined PDO/ENSO phases with different signs of ENSO. Furthermore, cold season precipitation is statistically similar during the coupled cycles with the same ENSO sign but statistically different among the combinations with opposite signs of ENSO (Fig. 8c) (C/C-W/W, W/C-W/W, W/C-C/W, and C/C-C/W with p-values: $3.7 \cdot 10^{-7}$, $9.6 \cdot 10^{-3}$, $2.4 \cdot 10^{-2}$, $3.8 \cdot 10^{-2}$, and $6.2 \cdot 10^{-5}$, respectively). These statistical differences show that the largest variability in cold season precipitation (expressed as% below or above the overall precipitation mean presented in Table 1) occur when both indicators are of same sign (C/C is 21.1% below the mean; W/W is 20% above the mean). Furthermore, ENSO largely dominates precipitation during the combined PDO/ENSO of opposite signs (W/C: 4.4% below the mean; C/W: 19.1% above the mean) (Fig. 6f, Table 1).

The warm season precipitation shows similar responses among all the coupled PDO/ENSO phases with similar medians and overlapping confidence intervals (Fig. 8d, Table 2). This along with the Mann-Whitney-Wilcoxon tests (p-values ranging from 0.2 to 0.9) confirm that there is no statistical difference among the data sets and, therefore, limited PDO/ENSO coupled influence on warm season precipitation variability is expected (Fig. 6f, Table 1).

3.4.2.2. Streamflow variability. Contrary to precipitation, the PDO/ENSO coupled effects on streamflow discharge do not seem to differ depending on the ENSO sign; the C/C, W/C, and C/W conditions show small differences in medians (Table 2) and a high degree of overlapping confidence intervals (Fig. 6f). However, a markedly high influence is shown when the two indices are on the positive phase (W/W). The Mann-Whitney-Wilcoxon test performed against all other conditions shows the following combinations to be statistically different: C/C-W/C, C/C-W/W, W/C-W/W, and W/C-W/W (p-values: $3.0 \cdot 10^{-3}$, $2.5 \cdot 10^{-16}$, $4.2 \cdot 10^{-9}$, and $1.5 \cdot 10^{-11}$). Annual streamflow variability estimates (expressed as% below or above the overall streamflow mean presented in Table 1) show strong influences of ENSO cold causing a decrease

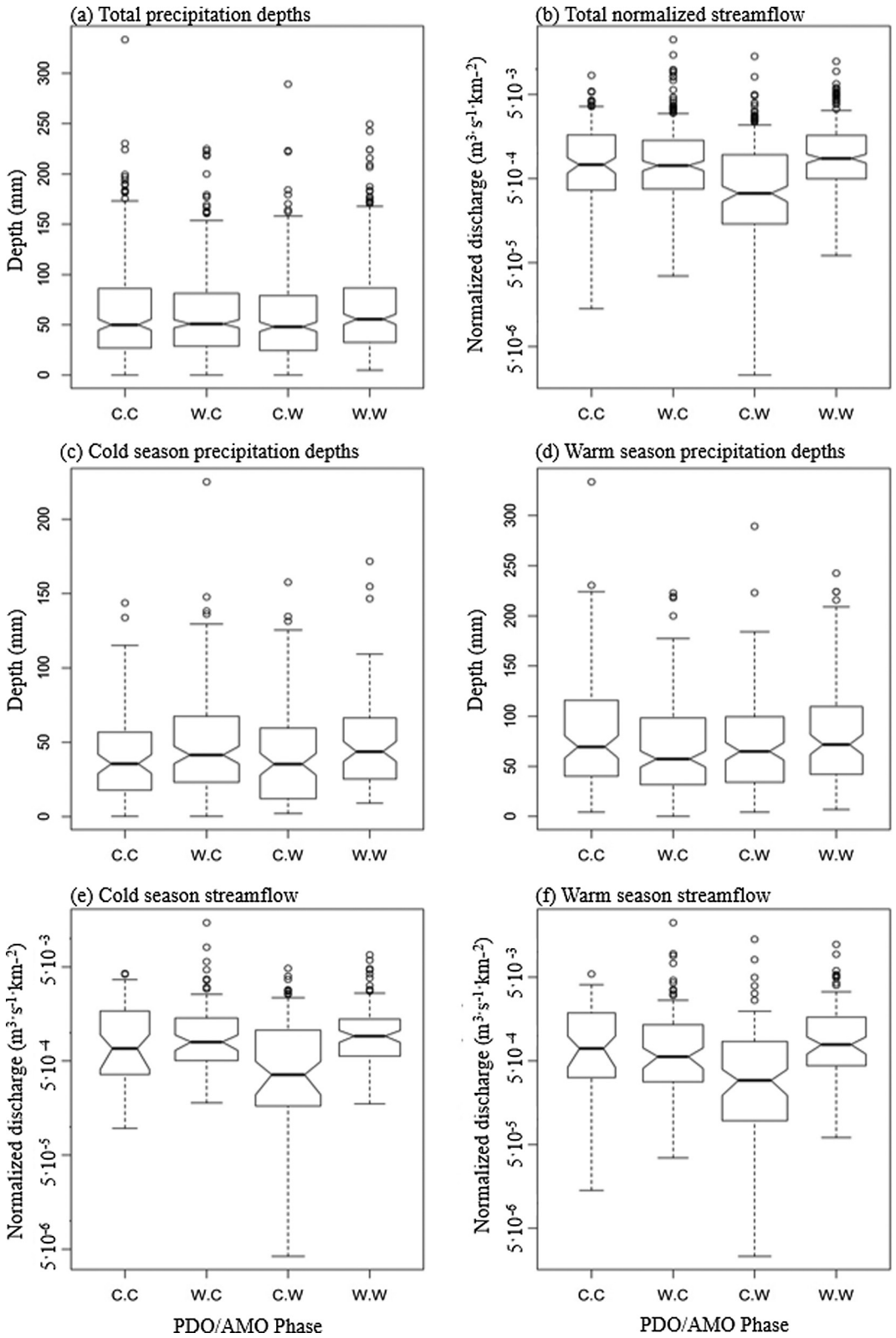

Fig. 7. Boxplot display of precipitation and streamflow for the different coupled PDO and AMO phases. The plots show differences in shape, spread as well as differences in medians and confidence intervals at the 95% for the mean monthly precipitation (a) and streamflow (b) records and for the different defined cold and warm seasons (d–f).

of discharge below the mean (C/C: 17.2% and W/C: 16.4%). On the other hand, the effects of ENSO warm, when streamflow is expected to increase, are overshadowed by the PDO in a negative phase causing a decrease of streamflow below the mean (C/W: 23.1%). A significant increase of streamflow above the mean occurs when both PDO and ENSO are in their positive phase (W/W: 42.5%) (Fig. 6f, Table 2).

There are small differences in medians for the cold and warm season streamflow during the coupled phases mentioned above with a distinctly higher median for the W/W (Fig. 8e; Table 1). This

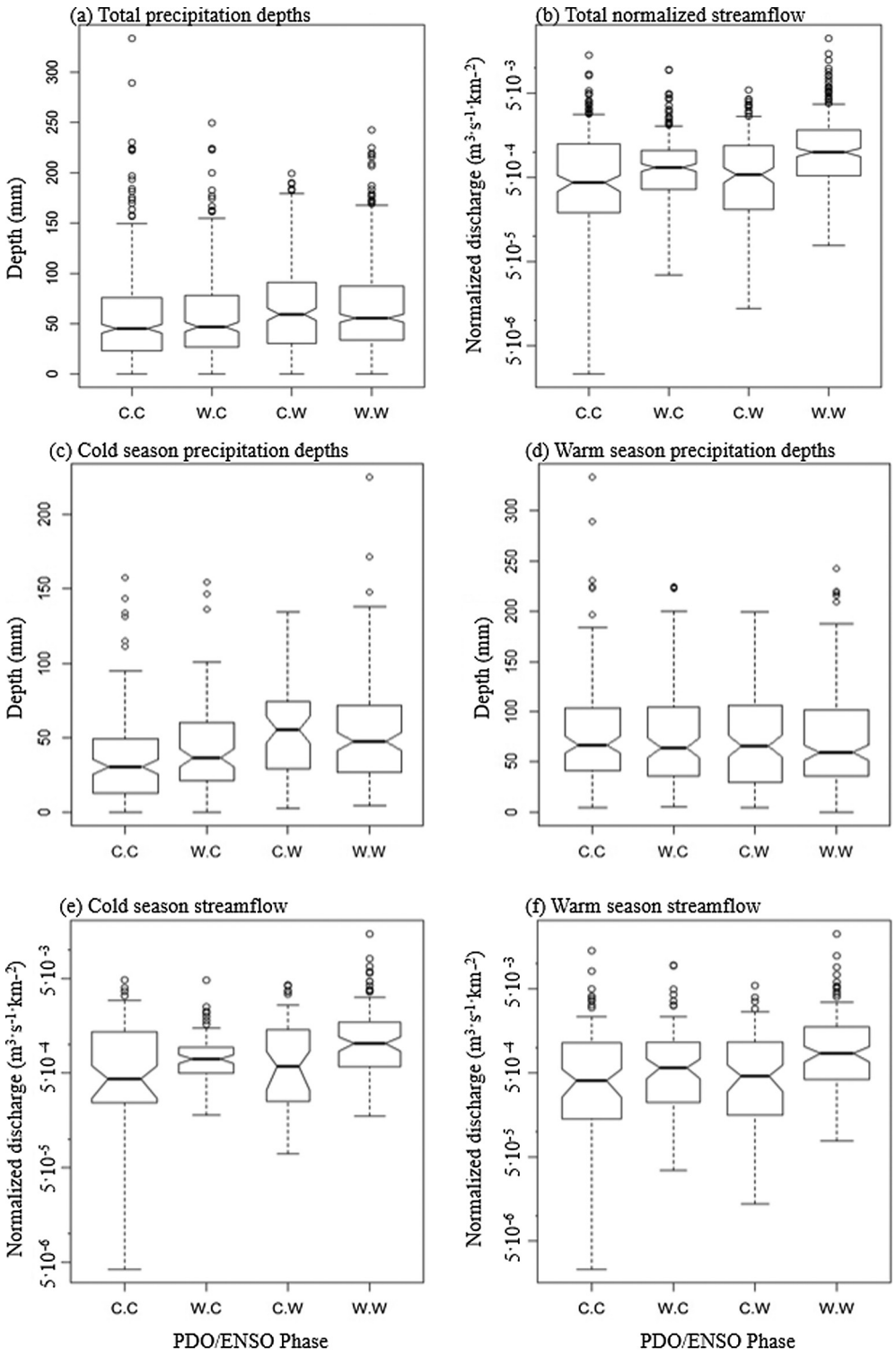

Fig. 8. Boxplot display of precipitation and streamflow for the different coupled PDO and ENSO phases. The plots show differences in shape, spread as well as differences in medians and confidence intervals at the 95% c.i. for the mean monthly precipitation (a) and streamflow (b) records and for the different defined cold and warm seasons (d–f).

results in the same significant difference combinations as for the annual streamflow, with p-values several orders of magnitude lower than 0.05 (i.e. $1.2 \cdot 10^{-6} \div 2.0 \cdot 10^{-3}$) and similar patterns of seasonal variabilities. The most significant variabilities are associated with the cold season streamflow when ENSO cold has a more dominant effect than PDO warm. On the other hand, PDO cold significantly lowers (21.4% below the mean) warm season streamflow during ENSO warm. Cold and warm streamflow increase considerably above the mean during (i.e. cold season mean) PDO and ENSO warm (Table 1, Fig. 6f), with a slightly higher effect on the cold season streamflow.

3.5. Drought analyses

Statistical analyses using the chi-squared and Cramer's "V" show that Texas droughts are strongly correlated with La Niña/El

Niño (V = 0.38) with La Niña playing the primary role (DS = 0.4; Fig. 3, Table 3). Our analyses show that PDO influences moderately the occurrence of droughts (V = 0.29) mostly during the cold phase, but likely intensifies the La Niña effects as indicated by the significant correlation with coupled PDO/ENSO (V = 0.36). As expected, the most severe droughts are occurring during the cold phases of both PDO and ENSO (DS = 0.6). These analyses also show that PDO warm could diminish the impacts of ENSO cold on droughts (DS = 1.3) while PDO cold intensifies droughts during ENSO warm (DS = 0.8) (Table 3). Although AMO has a very weak effect (V = 0.17), the warm phase is likely responsible for some of the droughts associated with South Texas (DS = 0.9) and may be intensifying the severity of droughts when overlapping with PDO cold (V = 0.35 for PDO/AMO). In fact, the effects of PDO cold, when coupled with AMO warm on the frequency and severity of droughts, are similar to those of La Niña, as shown by the same drought scores (0.4) (Table 3). A visual inspection of Texas droughts and climate indicators, depicted in Fig. 3, also indicate that droughts are more intense or frequent during the coupled PDO cold/AMO warm phases. For instance, the longest drought recorded in Texas occurred from 1950 to 1956 during the PDO/AMO C/W coupled phase. In addition, the highest frequency of recurring droughts starts with 1987 when AMO began its return to the warm phase and PDO intermittently switched from warm to cold phases.

4. Discussion

4.1. Climatic effects on South Texas precipitation and streamflow variability

In South Texas, significant differences are observed in rainfall amounts between the cold and warm seasons, with substantially higher precipitation during the warm season (~45 vs. ~75 mm). Differences in streamflow discharge between the two seasons are smaller with higher discharge during the warm season (warm and cold season: $1.13 \cdot 10^{-3}$ (n = 444) and $1.12 \cdot 10^{-3}$ $m^3 \cdot s^{-1} \cdot km^{-2}$, respectively). The results of this study show that although precipitation and streamflow are significantly positively correlated at zero lag and when precipitation leads streamflow by 1–8 months (Fig. 4), their responses to climatic influences are different (Figs. 6–8). The most significant climate influences on precipitation occur during the cold season with increases above the mean during ENSO- and PDO-warm and AMO-cold and decreases during ENSO- and PDO-cold and AMO-warm. There are very weak to- null effects on the warm season precipitation, when the largest amounts are delivered, suggesting that most of the rainfall variability in this area is related to the seasonal cycle rather than climatic anomalies. The lack of correlation between climatic variation and warm season precipitation may be due to increased evaporation rates overshadowing precipitation variability and driving the decrease of total available water (USGCRP, 2014).

In contrast to precipitation, SST anomalies have a strong influence on streamflow with significantly larger variabilities during both seasons. While feedbacks for cold season are expected to be in part due to changes in precipitation as modulated by the climatic anomalies the significant variability in the warm season streamflow points to a combination of other factors, including evaporation, water use and natural lags between precipitation and streamflow. Joseph et al. (2012) also suggests that while ENSO is expected to have more significant impacts in South Texas, during the most critical season, summer, PDO is more closely correlated to streamflow than is ENSO. As mentioned earlier, precipitation amounts are almost double during the warm season resulting in streamflow increases because of accumulation of seasonal rainfall and overland runoff in rivers. Precipitation that percolates into the aquifers during the warm season becomes discharge to rivers as baseflow that likely extends to the cold season (i.e. positive lagged correlations between 0 and -8 months as shown in Fig. 4) explaining the increase in streamflow during the cold season. High temperatures during the warm season generally result in a significant increase in evaporation rates (IPCC, 2007) especially in semi-arid to arid areas such as South Texas, where precipitation is exceeded almost twofold (SAR BBEST et al., 2011). A modest increase in average temperature can result in higher evaporation/evapotranspiration (ET) rates from soils reducing the amount available to plants, aquifer recharge, and hence streamflow. High rates of ET and groundwater use slowdown/reduce baseflow to streams and lead to lower stream levels (TPWD, 2017; USGCRP, 2014).

Spatial distribution of rainfall, evaporation rates, and water use likely further affect streamflow discharge in the area. As shown in Fig. 1, higher rainfall amounts are delivered in the eastern side of the area; whereas, the highest uses are located in the lower precipitation areas (i.e. San Antonio and Corpus Christi). Evaporation rates are also increasing from east to west along the climatic gradient. Lower precipitation amounts, high evaporation rates, and increased water uses will lead to a more substantial response of streamflow (i.e.% decrease) to climate factors as shown in this study. Alternatively, reallocation of water from headwater aquifers, the Edwards aquifer for instance, and delivery as treated municipal effluent, such as to the San Antonio River (see introduction section), amplifies streamflow discharge even when precipitation rates are lowest. Thus, the spatial distribution of rainfall, streamflow discharge, and water use, including groundwater, are substantially impacted by anthropogenic actions and are all-important factors to consider when analyzing the effects of SSTs on an area's climate, especially at sub-regional scales. We acknowledge, therefore, that the differences in precipitation and streamflow responses to climate anomalies is manifold as various factors involved in water management (many mentioned above)

Table 3
Contingency table summarizing drought months in Texas and the statistical significance (i.e. p-values) in relation to temporal phases of SSTs anomalies based on Chi squared tests. Presented are also the strength of correlation between drought months in Texas and the climate indicators given by Cramer's "V" values. Correlation of drought years with each temporal SST phase (e.g. PDO cold and warm) are inferred using the drought score and are marked with "*". Drought scores were not calculated for the PDO/La Niña or PDO/El Niño given the small sample size of each of the combinations (i.e. few overlapping months corresponding to drought events) also reflected by Cramer's "V" of 0.42 (worrisomely strong).

Climate indices	Non-drought months	Drought months	Drought Score (DS)
ENSO; p-value = 6.7^{-25}; V = 0.38			
La Niña (C)	89	218	*0.4
El Niño (W)	283	135	2.1
ENSO; p-value = $1.16 \cdot e^{-14}$; V = 0.21			
Cold	306	355	*0.9
Warm	450	219	2.1
PDO; p-value = $6.95e^{-26}$; V = 0.29			
Cold	243	360	*0.7
Warm	484	214	2.3
AMO; p-value = $1.34 \cdot e^{-9}$; V = 0.17			
Cold	470	261	1.8
Warm	286	313	*0.9
PDO/ENSO; p-value = $1.20 \cdot e^{-35}$; V = 0.36			
Cold/Cold	136	228	*0.6
Warm/Cold	160	127	1.3
Cold/Warm	107	132	*0.8
Warm/Warm	324	87	3.7
PDO/AMO; p-value = $1.31e^{-33}$; V = 0.35			
Cold/Cold	143	135	1.1
Warm/Cold	298	126	2.4
Cold/Warm	100	225	*0.4
Warm/Warm	186	88	2.1

could somewhat distort the relationship between climate anomalies and streamflow. The effects of these factors should be investigated in relation to climate anomalies for more robust conclusions.

4.2. Comparison with other studies

Other studies show a strong influence of ENSO on streamflow patterns over the western USA (Kahya and Dracup, 1993; Tootle et al., 2005), while PDO and AMO have only a weak influence on streamflow variability (Tootle et al., 2005). These studies are only in partial agreement with our findings, which show a strong influence of both ENSO and PDO on precipitation and streamflow and a weaker but potentially significant effect of AMO. Enfield et al. (2001) determined that during the AMO warm phase less than normal rainfall is occurring in most of the U.S. territory. Our results for streamflow are consistent with Enfield et al. (2001), but not the ones for precipitation. Tootle and Piechota (2006) indicate that during AMO-warm, Atlantic Ocean SSTs influence upper Mississippi River basin, peninsular Florida, and northwest U.S. streamflow. Additionally, the streamflow response to the AMO's shift in phase was shown to be obvious in the upper Mississippi River basin, the northern Rocky Mountain region, and upper Colorado River basin (Rogers and Coleman, 2003). Our findings show that although a shift to a warm/positive phase of AMO may have significant effects on the South Texas climate, it is the shifts in PDO-cold and warm phases that may have a stronger effect on the drought occurrence. Nevertheless, to our knowledge, there were no studies showing the effect of coupled PDO/AMO phases on climate conditions and water resources, at least for the southwest USA.

Similar to our findings, McCabe et al. (2004) estimated that more than 50% of the spatial and temporal variance in multidecadal drought frequency in the U.S. is attributed to PDO and AMO effects. The influence of PDO/AMO cycles on the occurrence of major droughts has also been noted by Hidalgo (2004) in the Yellowstone basin. In South Texas, increased intensity and frequency of droughts is related more specifically to the PDO/AMO C/W cycles, but a very strong relationship also is shown for the ENSO/La Niña events when also coupled with the cold phase of PDO. Furthermore, while other studies show that SSTs anomalies such as ENSO are responsible for higher variation in precipitation (i.e. up to 40% of annual precipitation) and less for changes in river discharge (i.e. up to 30%) (Sun and Furbish, 1997), our results show that in South Texas, ENSO, PDO and AMO are responsible for a greater response in streamflow discharge than precipitation, comparatively (Fig. 6). Although McCabe and Wolock (2014) show that temporal flow metrics in the US are only weakly associated with well-known climate indices, this study shows that at a subregional scale, streamflow may in fact show the greatest influence from SSTs anomalies, offering a better tool for predicting the impact on water resources when compared to precipitation.

5. Concluding remarks

Since water resources worldwide are affected by climate variability, there is a need to quantify these effects for robust water management decisions. This study applied a combination of statistical methods to quantify temporal variabilities in annual, warm season, and cold season precipitation/streamflow with large-scale climate phenomena such as ENSO, PDO, and AMO in a semi-arid region. We found a stronger modulation of ENSO on cold season precipitation and streamflow variability than during the warm season. Increases in precipitation above the mean are associated with the warm phases of ENSO, while decreases below the mean are characteristic of the cold phases. In contrast, streamflow is modulated almost equally by both ENSO warm and cold (with higher discharge rates during the warm phase and lower during the cold phase). Coupled analyses indicate that the effects of ENSO-cold are intensified by PDO-cold, resulting in much lower rainfall amounts during the cold season. On the other hand, there are strong teleconnections between PDO-warm and cold season streamflow during the ENSO-cold. PDO-cold/ENSO-warm has a strong influence on warm season streamflow although there is no significant modulation on precipitation depths. The highest mean precipitation of 82.6 mm or 38% above the overall study area mean was observed during the warm season when PDO and AMO are both in either their warm or cold phases. The highest mean streamflow of $16 \times 10^{-4}\ m^3 \cdot s^{-1} \cdot km^{-2}$ or 45% above the study area mean was observed during the coupled warm phases of the PDO and ENSO with no significant difference between the cold and warm season streamflows. The lowest mean precipitation of 35.4 mm or 41% below the overall mean of the study area was observed during the coupled cold phases of the PDO and ENSO while the lowest streamflow of $7.1 \cdot 10^{-4}\ m^3 \cdot s^{-1} \cdot km^{-2}$ or 35% below the study area mean was observed during the PDO-cold phase coupled with a warm AMO.

Although La Niña is responsible for drought occurrences in this area, PDO cold is the dominant driver when ENSO is in the warm phase. While no significant impact of AMO is observed on the area's precipitation depths, streamflow is consistently below the mean across the seasons and annually during PDO-cold/AMO-warm coinciding with the most intense and frequent droughts recorded in Texas for the investigated timeframe. At the investigated scales and for the climatic conditions on record, streamflow shows a strong correlation with SSTs anomalies. Such information is important when assessing and predicting our vulnerability to temporary or sustained scarcity risk of this water resource, especially with increasing temperatures, population and climate change. Consequently, streamflow offers a more direct tool for predicting impacts on water resources when compared to precipitation. However, we acknowledge that the cause of such significant correlations, as those observed in this study, is diverse and numerous factors involved in water management could influence the relationship between climate and streamflow. Although effects associated with water management practices and evaporation on water resources are not quantified herein, these statistical relations can provide water management decision makers with additional tools and knowledge to better assess current resources, while proactively mitigating future supply issues before they become further environmental and economic burdens within the study area and for other regions similar in nature.

Acknowledgments

This study was funded by the Center for Water Supply Studies, Texas A&M University-Corpus Christi. The authors thank the U.S. Geological Survey and the Texas Water Development Board for making their valuable data available. We would like to thank the reviewers for their insightful comments on the paper which led to an improvement of the work.

References

Anderson, O.D., 1977. Time series analysis and forecasting: another look at the Box-Jenkins approach. The Statistician: pp. 285–303.

Backlund, P., Janetos, A., Schimel, D., Walsh, M., 2008. The effects of climate change on agriculture, land resources, water resources, and biodiversity in the United States. The effects of climate change on agriculture, land resources, water resources, and biodiversity in the United States.

BEG, 2005. Groundwater-Surface Water Interaction in Texas. Bureau of Economic Geology.

Box, G.E.P., Jenkins, G.M., Reinsel, G.C., Ljung, G.M., 2015. Time Series Analysis: Forecasting and Control. John Wiley & Sons.

Chatfield, C., 2016. The Analysis of Time Series: An Introduction. CRC Press.

Clark, C., Nnaji, G.A., Huang, W.R., 2014. Effects of El-Nino and La-Nina sea surface temperature anomalies on annual precipitations and streamflow discharges in Southeastern United States. J. Coastal Res., 113–120 http://dx.doi.org/10.2112/SI68-015.1.
Cohen, J., 1988. Statistical Power Analysis for the Behavioral Sciences. Lawrence Erlbaum Associates, Hillsdale, NJ.
Cramér, H., 1946, Mathematical Methods of Statistics, Chapter s 21–24, 590.
Dai, A., Trenberth, K.E., New estimates of continental discharge and oceanic freshwater transport. In: Proceedings of the Symposium on Observing and Understanding the Variability of Water in Weather and Climate, 83rd Annual American Meteorological Society Meeting, Long Beach, CA, 2003, pp 1–18.
Day, J.W., Barras, J., Clairain, E., Johnston, J., Justic, D., Kemp, G.P., Ko, J.-Y., Lane, R., Mitsch, W.J., Steyer, G., 2005. Implications of global climatic change and energy cost and availability for the restoration of the Mississippi delta. Ecol. Eng. 24 (4), 253–265.
Döll, P., Fiedler, K., 2007. Global-scale modeling of groundwater recharge. Hydrol. Earth Syst. Sci. Discuss. 4 (6), 4069–4124.
Enfield, D.B., Mestas-Nuñez, A.M., Trimble, P.J., 2001. Evolution and historical perspective of the 1997–1998 El Nino-Southern Oscillation event. Bull. Mar. Sci. 69 (1), 7–25.
Faurès, J.-M., 1997. Indicators for sustainable water resources development. FAO Land and Water Bulletin (FAO).
Fisher, A., 1958. Statistical Methods and Research Workers. Hafner Publishing.
Fisher, A., 1973. Statistical Methods and Scientific Inference. Hafner Press.
Fu, G.B., Viney, N.R., Charles, S.P., Liu, J.R., 2010. Long-term temporal variation of extreme rainfall events in Australia: 1910–2006. J. Hydrometeorol. 11 (4), 950–965. http://dx.doi.org/10.1175/2010JHM1204.1.
Giorgi, F., Hewitson, B., Christensen, J., Hulme, M., Von Storch, H., Whetton, P., Jones, R., Mearns, L., Fu, C., Arritt, R., 2001. Regional climate information—evaluation and projections.
Gray, S.T., Graumlich, L.J., Betancourt, J.L., Pederson, G.T., 2004. A tree-ring based reconstruction of the Atlantic Multidecadal Oscillation since 1567 AD. Geophys. Res. Lett. 31 (12). doi:Artn L12205 10.1029/2004gl019932.
Hidalgo, H.G., 2004. Climate precursors of multidecadal drought variability in the western United States. Water Resour. Res. 40 (12). doi:Artn W12504 10.1029/2004wr003350.
Hidalgo, H.G., Dracup, J.A., 2001. Evidence of the signature of North Pacific multidecadal processes on precipitation and streamflow variations in the Upper Colorado River Basin. In: Paper Presented at the 6th Biennial Conference of Research on the Colorado River Plateau.
Hidalgo, H.G., Dracup, J.A., 2003. ENSO and PDO effects on hydroclimatic variations of the Upper Colorado River basin. J. Hydrometeorol. 4 (1), 5–23. http://dx.doi.org/10.1175/1525-7541(2003) 004<0005:Eapeoh>2.0.Co;2.
Hyndman, R., 2008. Forecasting Functions for Time Series: R Package Version 2.13. URL <http://CRAN R-project org/package= forecasting>.
IPCC, I.P.O.C.C., 2007. Climate change 2007: impacts, adaptation and vulnerability. Genebra, Suíça.
Jensen, R., 1996. Why droughts plague Texas. Texas Water Resour. 22 (2).
Joseph, J.F., Falcon, H.E., Sharif, H.O., 2012. Hydrologic trends and correlations in south Texas River basins: 1950–2009. J. Hydrol. Eng. 18 (12), 1653–1662.
Kahya, E., Dracup, J.A., 1993. United-States streamflow patterns in relation to the El-Nino southern oscillation. Water Resour. Res. 29 (8), 2491–2503. http://dx.doi.org/10.1029/93wr00744.
Kaplan, A., Cane, M.A., Kushnir, Y., Clement, A.C., Blumenthal, M.B., Rajagopalan, B., 1998. Analyses of global sea surface temperature 1856–1991. J. Geophys. Res-Oceans 103 (C9), 18567–18589. http://dx.doi.org/10.1029/97jc01736.
Karl, T.R., 2009. Global Climate Change Impacts in the United States. Cambridge University Press.
Kim, J.Y., Lee, H., Lee, J.E., Chung, M.-S., Ko, G.P., 2013. Identification of human and animal fecal contamination after rainfall in the Han River, Korea. Microb. Environ. 28 (2), 187–194.
Kuss, A.J.M., Gurdak, J.J., 2014. Groundwater level response in US principal aquifers to ENSO, NAO, PDO, and AMO. J. Hydrol. 519, 1939–1952.
Mantua, N.J., Hare, S.R., Zhang, Y., Wallace, J.M., Francis, R.C., 1997. A Pacific interdecadal climate oscillation with impacts on salmon production. Bull. Am. Meteorol. Soc. 78 (6), 1069–1079. http://dx.doi.org/10.1175/1520-0477(1997)078<1069:Apicow>2.0.Co;2.
Maurer, E.P., Lettenmaier, D.P., Mantua, N.J., 2004. Variability and potential sources of predictability of North American runoff. Water Resour. Res. 40 (9). doi:Artn W09306 10.1029/2003wr002789.
McCabe, G.J., Palecki, M.A., Betancourt, J.L., 2004. Pacific and Atlantic Ocean influences on multidecadal drought frequency in the United States. Proc. Natl. Acad. Sci. U.S.A. 101 (12), 4136–4141. http://dx.doi.org/10.1073/pnas.0306738101.
McCabe, G.J., Wolock, D.M., 2014. Spatial and temporal patterns in conterminous United States streamflow characteristics. Geophys. Res. Lett. 41 (19), 6889–6897. http://dx.doi.org/10.1002/2014GL061980.
Meixner, T., Manning, A.H., Stonestrom, D.A., Allen, D.M., Ajami, H., Blasch, K.W., Brookfield, A.E., Castro, C.L., Clark, J.F., Gochis, D.J., 2016. Implications of projected climate change for groundwater recharge in the western United States. J. Hydrol. 534, 124–138.
Nist/Sematech, 2012. Chi-square goodness-of-fit test, in Electronic-Handbook of Statistical Methods.
Norwine, J., Giardino, J R., North, G.R., Veldes, J.B., 1995. The Changing Climate of Texas: Predictability and Implications for the Future. College Station, TX: Cartographics, Texas A&M University: pp. 138–154.
Pachauri, R.K., Allen, M.R., Barros, V., Broome, J., Cramer, W., Christ, R., Church, J., Clarke, L., Dahe, Q., Dasgupta, P., 2014. Climate change 2014: synthesis Report. Contribution of working groups I, II and III to the fifth assessment report of the intergovernmental panel on climate change. IPCC.
Parry, M.L., 2007. Climate Change 2007-Impacts, Adaptation and Vulnerability: Working Group II Contribution to the Fourth Assessment Report of the IPCC, vol 4. Cambridge University Press.
Prathumratana, L., Sthiannopkao, S., Kim, K.W., 2008. The relationship of climatic and hydrological parameters to surface water quality in the lower Mekong River. Environ. Int. 34 (6), 860–866.
Reynolds, R.W., Smith, T.M., 1994. Improved global sea-surface temperature analyses using optimum interpolation. J. Clim. 7 (6), 929–948. http://dx.doi.org/10.1175/1520-0442(1994) 007<0929:Igssta>2.0.Co;2.
Rogers, J.C., Coleman, J.S.M., 2003. Interactions between the Atlantic Multidecadal Oscillation, El Nino/La Nina, and the PNA in winter Mississippi valley stream flow. Geophys Res Lett 30 (10). doi:Artn 1518 10.1029/2003gl017216.
Salas, J., Delleur, J., Yevjevich, V., Lane, W., 1980. Applied Modeling of Hydrologic Time Series. Water Resor. Pub, Littleton, CO, USA.
SAR BBEST, G., San Antonio, Mission, and Aransas Rivers and Mission, Copano, Aransas, and San Antonio Bays Basin and Bay Expert Science Team., 2011. Environmental Flows Recommendations Report. 152.
Snedecor, G.W., Cochran, W.G., 1989. Statistical Methods. Iowa State University Press.
Sun, H.B., Furbish, D.J., 1997. Annual precipitation and river discharges in Florida in response to El Nino and La Nina sea surface temperature anomalies. J. Hydrol. 199 (1–2), 74–87. http://dx.doi.org/10.1016/S0022-1694(96)03303-3.
Taylor, R.G., Scanlon, B., Döll, P., Rodell, M., Van Beek, R., Wada, Y., Longuevergne, L., Leblanc, M., Famiglietti, J.S., Edmunds, M., 2013. Ground water and climate change. Nat. Clim. Change 3 (4), 322–329.
Tootle, G.A., Piechota, T.C., 2006. Relationships between Pacific and Atlantic ocean sea surface temperatures and US streamflow variability. Water Resour. Res. 42 (7). doi: Artn W07411 10.1029/2005wr004184.
Tootle, G.A., Piechota, T.C., Singh, A., 2005. Coupled oceanic-atmospheric variability and U.S. streamflow. Water Resour. Res. 41 (12). doi: Artn W12408 10.1029/2005wr004381.
TPWD, 2017. The State of Water in the South Texas Brush Country. Texas Parks and Wildlife.
Trenberth, K.E., 1997. The definition of El Nino. Bull. Am. Meteorol. Soc. 78 (12), 2771–2777. http://dx.doi.org/10.1175/1520-0477(1997) 078<2771:Tdoeno>2.0.Co;2.
TWDB, T.W.D.B., 1996. River basin map of Texas, Bureau of Economic Geology, the University of Texas at Austin. 2.
TWDB, T.W.D.B., 2012. Water for Texas 2012 State Water Plan. 145–155.
TWRI, T.W.R.I., 2011. Texas drought: now and then. vol 7, number 1. Texas Water Resources Institute, Texas AgriLife Research, Kathy Wythe Ed.
USGCRP, 2014. Shafer, M., Ojima, D., Antle, J.M., Kluck, D., McPherson, R.A., Petersen, S., Scanlon, B., Sherman, K., 2014: Ch 19: Climate change impacts in the United States: the third national climate assessment, McKibben, Bill. New York Review 1755 Broadway, 5th Floor, New York, NY 10019 USA.
Wolock, D.M., McCabe, G.J., 1999. Estimates of runoff using water-balance and atmospheric general circulation models1. JAWRA J. Am. Water Resour. Assoc. 35 (6), 1341–1350.